Supplementary Material

Symmetry-Broken FeN_3–O on a Negatively Charged Carbon Host: Dual Modulation of Electronic Structure and Interfacial Field for Robust Oxygen Reduction

Yan Liu [a,*], Zhaoyu Wang [b], Shixiu Cao [c], Fuzhu Liu [a], Qiang Tan [a], Yuanzhen Chen [a], and Wei Wang [a]

[a] *State Key Laboratory for Mechanical Behavior of Materials, Xi'an Jiaotong University, Xi'an 710049, China*

[b] *Frontier Institute of Science and Technology, Xi'an Jiaotong University, Xi'an 712046, China*

[c] *Chongqing University Key Laboratory of Micro/Nano Materials Engineering and Technology, Chongqing University of Arts and Sciences, Yongchuan, Chongqing 402160, China*

*Corresponding author.

Email addresses: liuyan19@xjtu.edu.cn (Y. Liu)

Figure and Table Captions:

Experimental Section

Materials and reagents

The following reagents were sourced as follows: Colloidal silica (Ludox HS-30, 30%), aniline (C_6H_7N, with an analytical reagent grade of ≥98.0%), ammonium persulfate ($(NH_4)_2S_2O_8$, analytical reagent grade ≥98%), and sodium hydroxide (NaOH, analytical reagent grade ≥96.0%) were procured from Sigma-Aldrich in Shanghai, China. N, N-methylene bisacrylamide ($C_7H_{10}N_2O_2$, analytical reagent grade ≥99.0%) and acrylic acid ($C_3H_4O_2$, analytical reagent grade ≥99.5%) were acquired from Kemiou Chemical Reagent Co., Ltd in Tianjin, China. Pt/C (HiSPEC 4000, 40 wt.%) was obtained from Johnson Matthey. The polytetrafluoroethylene solution (PTFE, 60%) was supplied by 3F New Materials Co., Ltd in Shanghai, China. The gas diffusion layers were sourced from Sipulin New Energy Technology Co., Ltd in Changsha, China. All the reagents were utilized without any further alteration or purification.

Characterization of catalysts

The structural characteristics of the catalysts were investigated via X-ray diffraction (XRD, X'Pert PRO), with Cu Kα radiation serving as the X-ray source. The morphologies and microstructures of the materials were appraised by means of a field-emission scanning electron microscope (FE-SEM, JSM-6700F, JEOL, Japan), a transmission electron microscope (TEM), and a high-resolution TEM (HRTEM) (JEOL JEM-F200 (HR), Japan). The HAADF-STEM images and corresponding EDS mapping

images were acquired via a FEI Themis Z. Raman spectra were documented using Raman microscopes (HORIBA) under 532 nm laser excitation. The specific surface areas, calculated according to the Brunauer-Emmett-Teller (BET) model, and the pore sizes, determined by the Density Function Theory (DFT) method, of the samples were gauged on an ASAP 2460 gas porosimeter (Micromeritics). The elemental composition and chemical states of the materials were ascertained by X-ray photoelectron spectroscopy (XPS) employing an ESCALAB Xi^+ instrument (Thermo Fisher Scientific) with Al Kα as the X-ray source. The binding energies were calibrated relative to the C 1s peak at 284.8 eV.

The X-ray absorption fine structure (XAFS) analyses of the materials were carried out as follows. Fe *K*-edge analysis was executed with Si (111) crystal monochromators at the BL14W1 beamlines of the Shanghai Synchrotron Radiation Facility (SSRF, Shanghai, China). Prior to the analysis at the beamline, the samples were compressed into thin sheets with a diameter of 1 cm and sealed with Kapton tape film. The XAFS spectra were recorded at room temperature using a 4-channel Silicon Drift Detector (SDD) Bruker 5040. The Fe *K*-edge extended X-ray absorption fine structure (EXAFS) spectra were recorded in transmission mode. Negligible alterations in the line shape and peak position of the Fe *K*-edge XANES spectra were detected between two scans for a particular sample. The XAFS spectra of these standard samples (Fe foil and FePc) were also recorded in transmission mode. The spectra were processed and analyzed with the software programs Athena and Artemis.

Electrochemical measurements

The electrochemical properties of the catalysts we fabricated were evaluated using an electrochemical workstation (CHI 750D, CH Instruments) within a three-electrode system that was interfaced with a Modulated Speed Rotator (Pine instrument). The three-electrode cell comprised a glassy carbon-based rotating disk electrode (RDE, with a diameter of 5 mm and an area of 0.196 cm^2) functioning as the working electrode, a Hg/HgO (1 M KOH) reference electrode, and a carbon counter electrode. The reference electrode was calibrated against the reversible hydrogen electrode (RHE) by immersing a calibration tube containing a Pt wire in a H_2 gas-purged 0.1 M KOH solution.

To prepare a working electrode, the catalyst ink was fabricated in the following manner. Initially, 2 mg of each catalyst was immersed and uniformly dispersed within a mixture comprising 100 μL of distilled water, 250 μL of ethanol, and 10 μL of Nafion solution (5 wt.%) by sonicating for one hour. Subsequently, 10 μL of the homogeneous black ink was extracted by two times and deposited onto the glassy carbon surface of a Rotating Disk Electrode (RDE), followed by natural drying. The loading amount of the catalyst was computed to be 0.283 mg cm^{-2}. Pt/C (40 wt.%) was chosen for a comparison employing the following ink ratios: 2 mg of Pt/C was thoroughly dispersed by ultrasonication in a solution constituted of 2 mL of ethanol and 20 μL of Nafion solution (5 wt.%). The loading of Pt/C was determined to be 0.0756 mg cm^{-2}.

Cyclic voltammetry (CV) curves were acquired in O_2- and N_2-saturated 0.1 M KOH solutions, with a sweep rate set at 50 mV s^{-1}. Linear scan voltammetry (LSV) was documented at a scan rate of 10 mV s^{-1} in an O_2-saturated 0.1 M KOH solution, employing a Rotating Disk Electrode (RDE) at various rotational speeds. The stability of the catalysts, as gauged by chronoamperometric responses, along with the alterations in current density upon the addition of methanol, were quantified in an O_2-saturated 0.1 M KOH solution at a rotation rate of 1200 rpm and a potential of 0.88 V. All the experimental procedures were executed at ambient temperature.

The electron transfer number (n) involved in ORR is calculated based on Koutechy-Levich (K-L) equations:

$$\frac{1}{J} = \frac{1}{J_k} + \frac{1}{B\omega^{1/2}} \quad (1)$$

$$B = 0.62nFD_0^{2/3}\upsilon^{-1/6}C_0 \quad (2)$$

Where J is the measured current density, J_k is the kinetic current density, ω is the angular velocity (rad), n is the electron transfer number, F is the Faraday constant (96500 C mol-1), Do is the diffusion coefficient of O_2 in 0.1 M KOH (1.9×10^{-5} cm^2 s^{-1}), C_o is the bulk concentration of O_2 (1.2×10^{-6} mol cm^3), and ν is the viscosity of the electrolyte (1.0×10^{-2} cm^2 s^{-1}).

The electrochemical double-layer capacitance (C_{dl}) value was obtained by the CV curves obtained at different scan rates in the non-Faraday zone, which can be calculated by the equation:

$$C_{dl} = \frac{j_a - j_c}{2 \times v} \tag{3}$$

where j_a and j_c is the anodic and cathodic current density, respectively, recorded at the middle (1.15 V vs. RHE) of the selected potential range, and v is the scan rate.

Zeta Potential Measurement: Disperse 3 mg of the catalyst powder in 10 mL of deionized water. After ultrasonication, pipette 1 mL of the resulting suspension for zeta potential measurement.

Experimental Procedure for Evaluating Resistance to H_2O_2 Poisoning: First, perform linear sweep voltammetry (LSV) measurements on the catalyst-coated disk electrode in 0.1 M KOH electrolyte. Then, replace the test electrolyte with a mixed solution of 0.1 M KOH and 0.5 mM H_2O_2, and conduct chronoamperometric response measurements at a potential of 0.5 V vs. RHE for 20 minutes. After the chronoamperometric test, gently rinse the electrode surface with deionized water, and then place the electrode back into the 0.1 M KOH electrolyte for a second round of LSV measurements. For all the aforementioned LSV measurements, the scan rate is set at 10 mV/s and the rotation speed of the working electrode is maintained at 900 revolutions per minute (rpm).

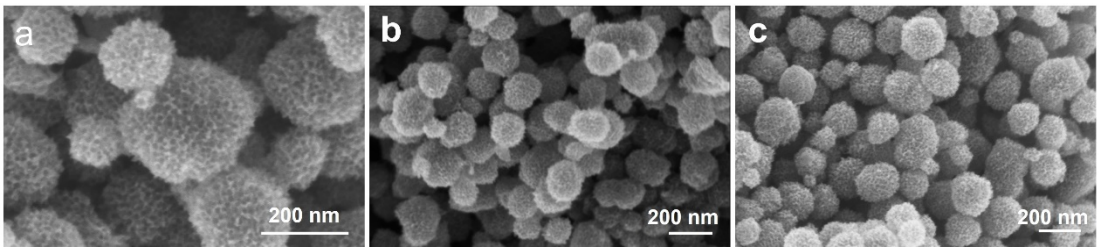

Figure S1. SEM images of a) HPCS, b) E-FeN$_3$-O/HPCS-1 and c) E-FeN$_3$-O/HPCS-3.

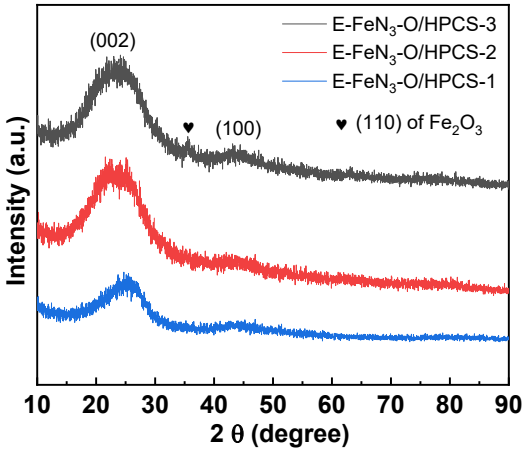

Figure S2. XRD patterns of the catalysts.

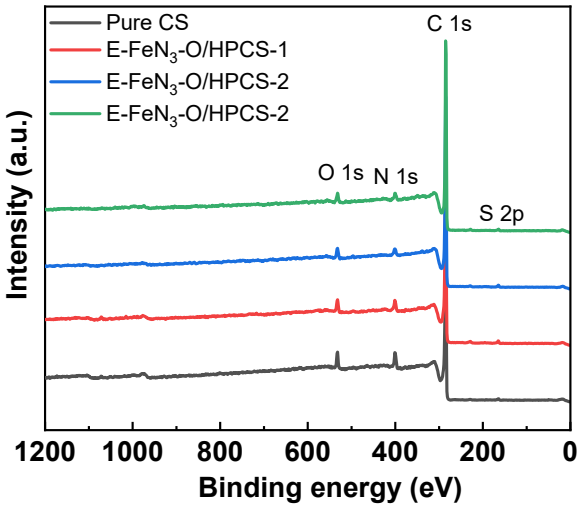

Figure S3. XPS survey spectra of the catalysts.

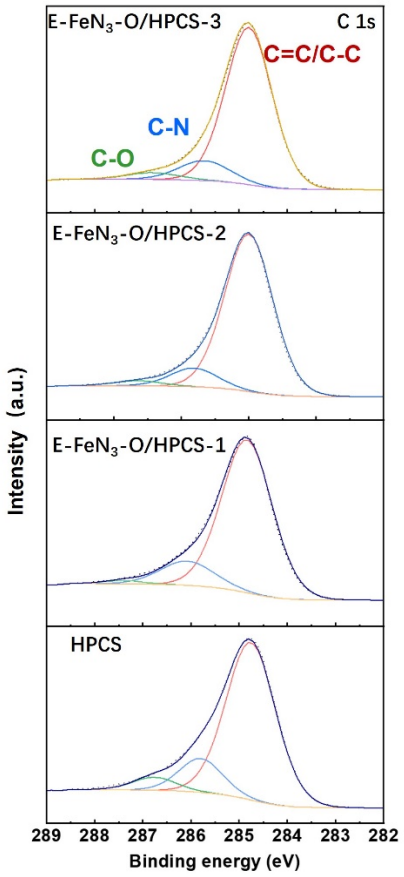

Figure S4. High-resolution XPS spectra of C 1s.

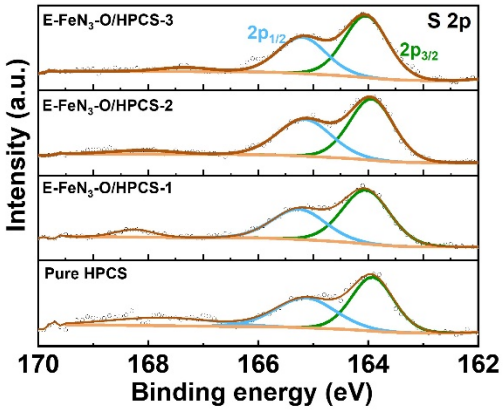

Figure S5. High-resolution XPS spectra of S 2p.

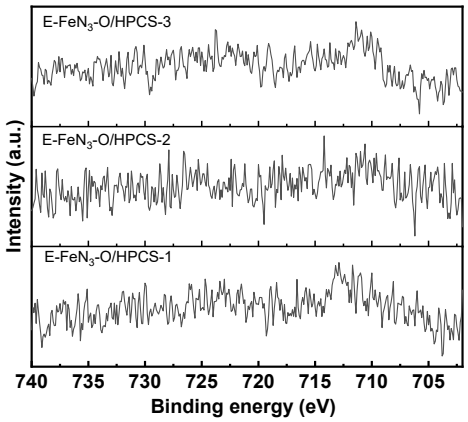

Figure S6. High-resolution XPS spectra of Fe 2p.

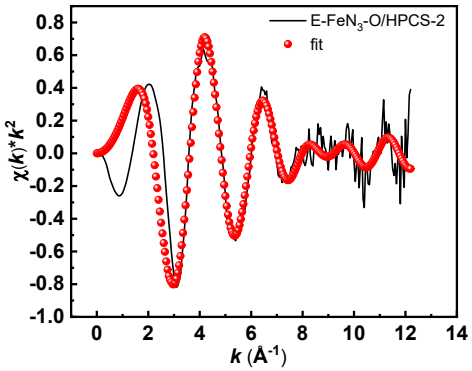

Figure S7. Fe K-edge EXAFs (points) and curve fit (line) for E-FeN_3-O/HPCS-2, shown in *k*-space. The data are k^2-weighted.

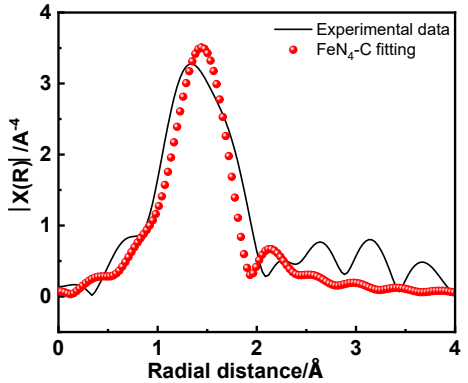

Figure S8. FT-EXAFS fitted curves of FeN_4-C at the Fe K-edge, shown in R space.

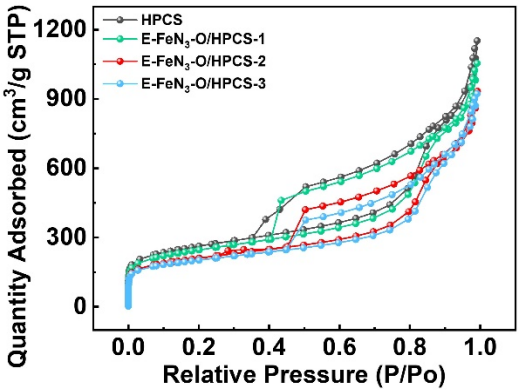

Figure S9. N_2 adsorption-desorption isotherm.

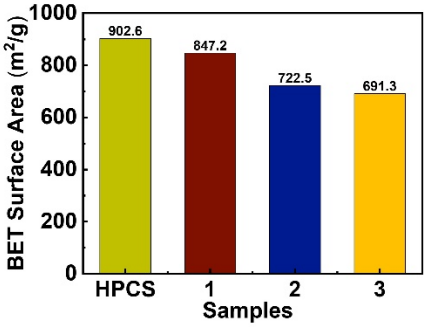

Figure S10. BET surface area of the samples. (1: E-FeN_3-O/HPCS-1. 2: E-FeN_3-O/HPCS-2. 3: E-FeN_3-O/HPCS-3.)

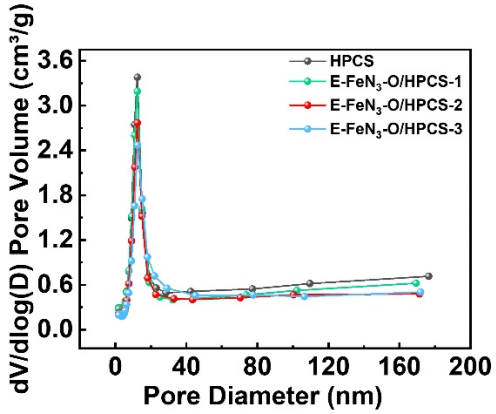

Figure S11. Pore width distribution curves of the samples.

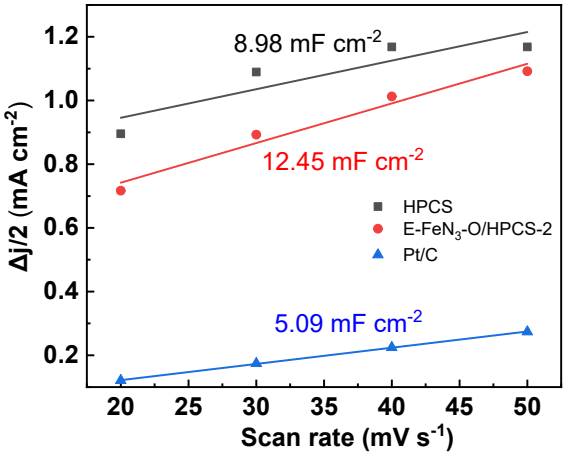

Figure S12. Current density difference (Δj) at 1.15 V versus RHE plotted against scan rates of various samples.

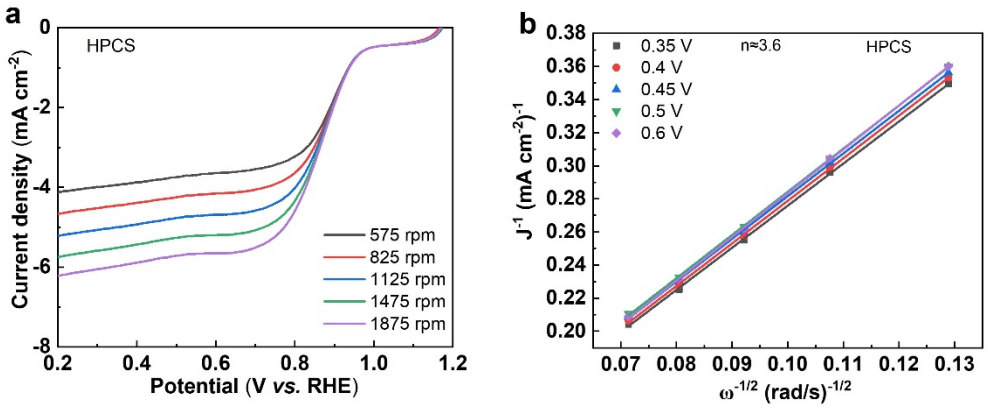

Figure S13. a) LSV polarization curves at different rotating rates for HPCS in oxygen-saturated 0.1 M KOH. b) corresponding Koutecky–Levich plots at different potentials of HPCS.

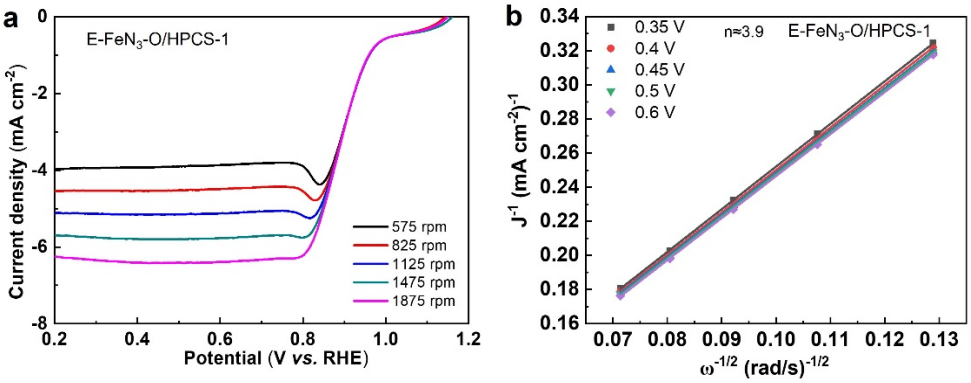

Figure S14. a) LSV polarization curves at different rotating rates for E-FeN_3-O/HPCS-1 in oxygen-saturated 0.1 M KOH. b) corresponding Koutecky–Levich plots at different potentials of E-FeN_3-O/HPCS-1.

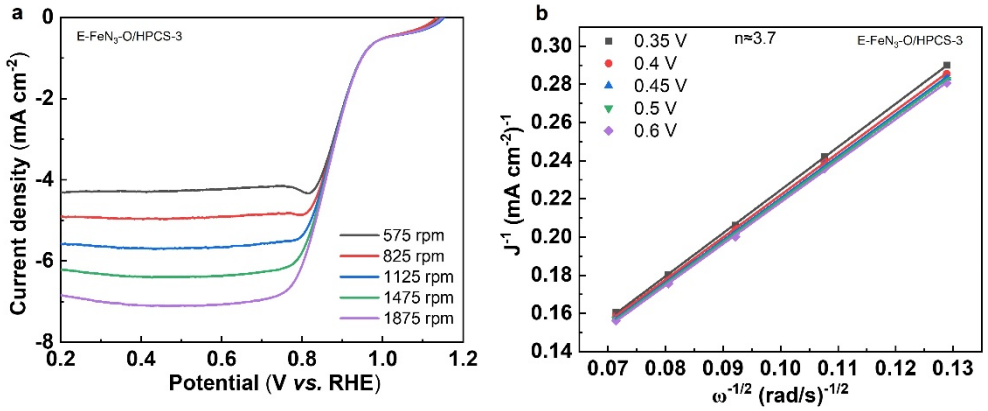

Figure S15. a) LSV polarization curves at different rotating rates for E-FeN_3-O/HPCS-3 in oxygen-saturated 0.1 M KOH. b) corresponding Koutecky–Levich plots at different potentials of E-FeN_3-O/HPCS-3.

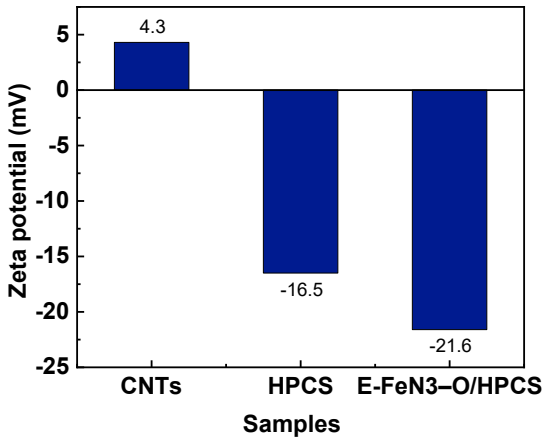

Figure S16. The values of Zeta potential of the samples dispersed in distilled water.

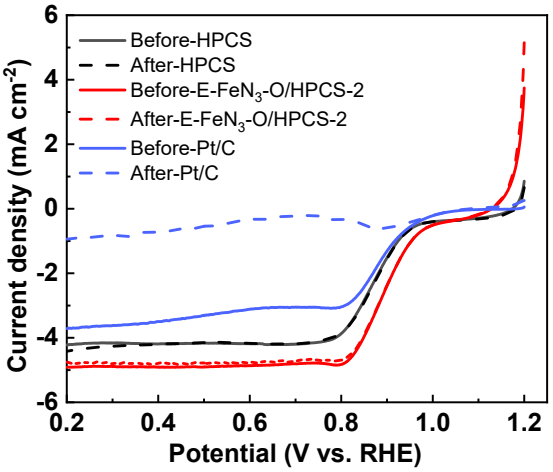

Figure S17. LSV curves of different samples before and after H_2O_2 poisoning. rotating rate: 900 rpm.

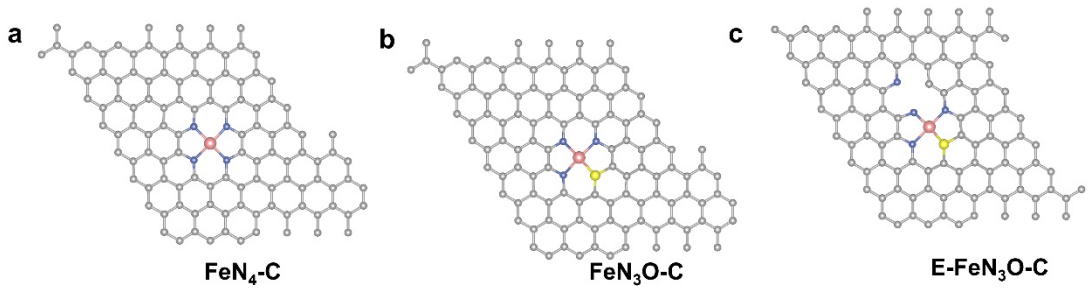

Figure S18. The optimized stable structures of FeN_4/C, FeN_3O/C and E-FeN_3O/C.

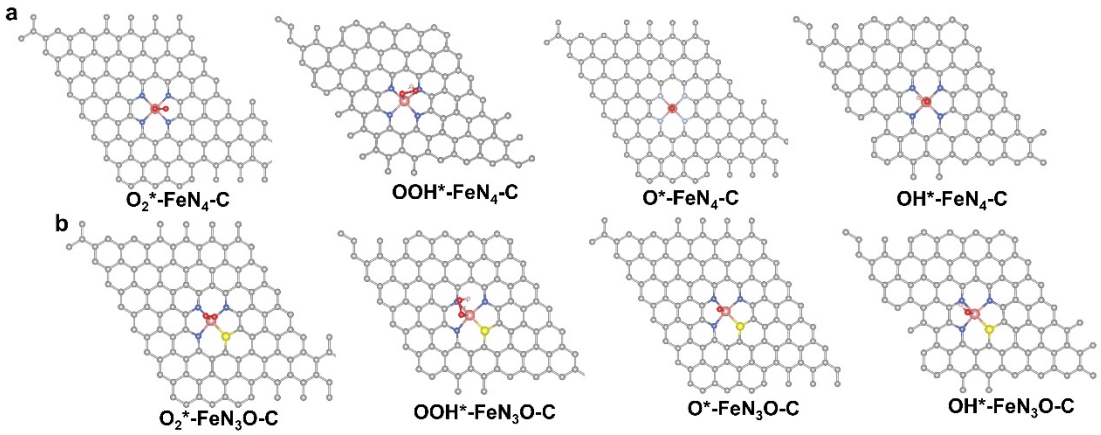

Figure S19. The structural optimization models for the adsorption of reaction intermediates on a) FeN_4-C and b) FeN_3O-C.

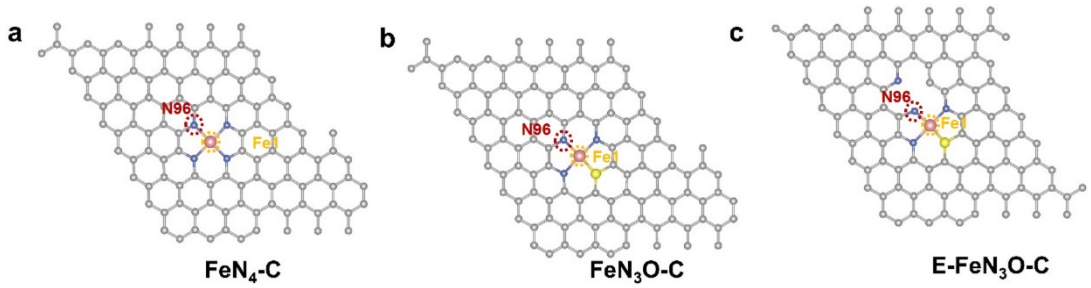

Figure S20. Atomic positions for orbital hybridization analysis (N96 and Fe1 denote the atomic indices of the nitrogen and iron atoms in the full structure, respectively).

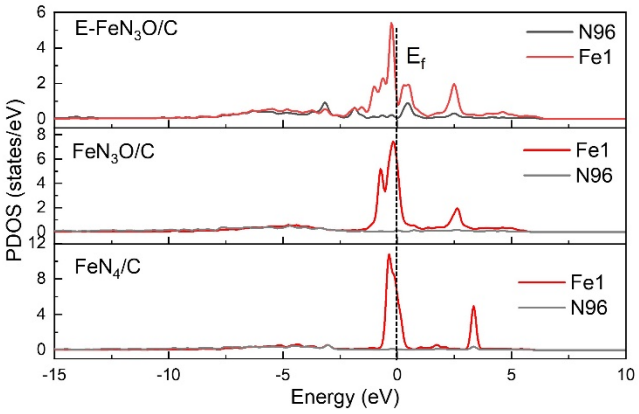

Figure S21. Partial density of states calculation for a single atom.

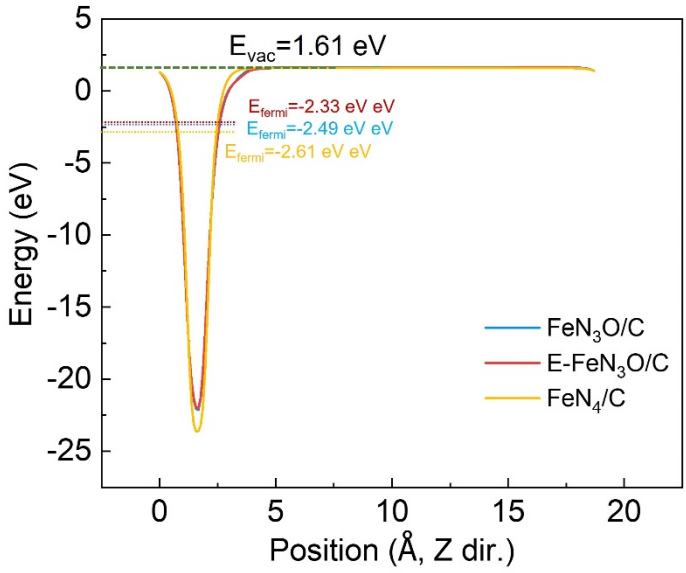

Figure S22. Calculations of electrostatic potential and work function for different structures.

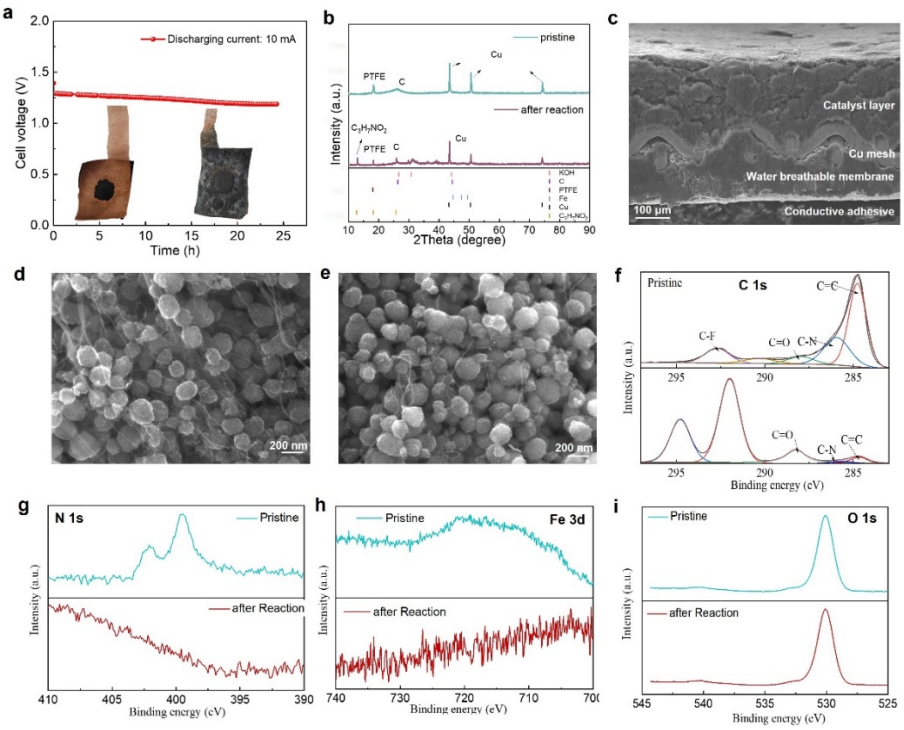

Figure S23. a) Discharge stability of the oxygen-air electrode (inset: digital photos of the electrode before and after the reaction). b) XRD patterns of the electrode before and after the reaction. Figure c) Cross-sectional image of the electrode. d) and e) FE-SEM images of the electrode before and after the reaction. f–i) XPS spectra of the electrode before and after the reaction.

Table S1. The iron content in each sample measured via ICP-MS.

Samples	Elemental concentrations of the tested solution (ug/L)	The elemental concentration of the original digestion solution/C_1(ug/L)	The elemental content of the sample/C_x (ug/kg)	The elemental content of the sample/W (%)
1	51.061	5106.13593	5526121.1	0.55%
1	51.125	5112.48413	5532991.5	0.55%
2	69.267	6926.71475	8017031.0	0.80%
2	69.284	6928.39677	8018977.7	0.80%
3	161.823	16182.2784	17666242.8	1.77%
3	160.396	16039.5977	17510477.8	1.75%

Note: 1: E-FeN_3-O/HPCS-1. 2: E-FeN_3-O/HPCS-2. 3: E-FeN_3-O/HPCS-3.

Table S2. Peaks splitting of the high-resolution N 1s spectra in the samples.

Samples	Peak（eV）	Peak 2（eV）	Peak 3（eV）	Peak 4（eV）
HPCS	398.4	400.1	401.08	402.4
E-FeN_3-O/HPCS-1	398.3	399.6	401.0	402.9
E-FeN_3-O/HPCS-2	398.3	399.41	401.01	402.7
E-FeN_3-O/HPCS-2	398.3	399.56	401.0	402.5

Table S3. Curve fit parameters[a] for Fe K-edge EXAFS based on E-FeN_3-O/HPCS structure.

Path	N[b]	R/Å	δ^2/ Å^2
Fe-N	3.2	1.899	0.018
Fe-O	0.8	2.196	0.00035

[a] S_0^2 was fitting based on Fe foil as 1.0. The inner potential correction (ΔE_0) is 12 eV. Data ranges: $3 \leq k \leq 10.241$, $1 \leq R \leq 3$. The number of variable parameters is 7, out of a total of 8.94 independent data points. R-factor for this fit is 0.02. Reduced chi-space for this fit is 235.08.

[b] These coordination numbers were constrained as N (Fe-N) = 3.3 and N (Fe-O) = 0.7 based on the standard structure.

Table S4. Curve fit parameters[a] for Fe K-edge EXAFS based on FeN_4-C structure.

Path	N[b]	R/Å	δ^2/ Å^2
Fe-N	4.01	1.96	0.008

[a] S_0^2 was fitting based on Fe foil as 1.3. The inner potential correction (ΔE_0) is 4.8 eV. Data ranges: $3 \leq k \leq 10.24$, $1.3 \leq R \leq 2.6$. The number of variable parameters is 4, out of a total of 5.73 independent data points. R-factor for this fit is 0.02. Reduced chi-space for this fit is 229.36.

[b] These coordination numbers were constrained as N (Fe-N) = 4.01 based on the standard structure.